Detection and characterization of anelastic AVF with the Gabor transform

Jesse M. Kolb, Kristopher A. H. Innanen

ABSTRACT

Amplitude variation with frequency (AVF) inversion can be used to estimate Q given anelastic frequency-dependent reflection coefficients. While AVF signal is generally analyzed event-by-event, traces are usually populated with many events at different arrival times. This creates the need to perform time-frequency analysis in order to isolate the reflectivity from a single event. We choose the Gabor transform as the instrument for our analysis and use it to estimate frequency-dependent reflectivities from synthetic traces. These reflectivities are then inverted to obtain accurate Q estimates. In order to test limits of this method, we also tested its performance under increasing noise levels, as well as with a reflection from a second interface that is close to the interface in which we are interested.

INTRODUCTION

Accurate estimation of the seismic quality factor Q is valuable for a number of reasons including allowing for inverse Q filtering (Hargreaves and Calvert, 1991), which yields better results for amplitude analysis, as well as indicating fluid properties such as fluid saturation (e.g. Kuster and Toksöz, 1974; Mavko and Nur, 1979), permeability (for a review, see Pride et al., 2003), and viscosity (e.g. Vasheghani and Lines, 2009).

A number of methods exist for estimating Q, and Cheng and Margrave (2012) recently reviewed a few of the more common ones in a CREWES report. Most methods for Q estimation involve analyzing propagation effects of Q, while AVF is different in that it analyzes Q's effects on reflection coefficients. Bird (2012) used the fast S-transform to estimate Q, but the method had difficulty estimating low frequency content from a single event when there are multiple events in a trace, due to the large window size used for low frequencies.

As an alternative to the S-transform for AVF analysis, we tested the Gabor transform, in the hope of being able to better isolate events by not using large window sizes. Using smaller window sizes can have negative effects (see the "close reflectors" section in which we vary the window size for more information), but we still find that the Gabor transform is able to accurately estimate Q for our synthetic data.

ESTIMATING R(ω) AND Q WITH THE GABOR TRANSFORM

For the tests in this report, synthetic traces from multi-layered velocity and Q models were created in the frequency domain. To model attenuation and dispersion we modified the wavenumber, k, to a model described by Aki and Richards (2002) for nearly constant Q:

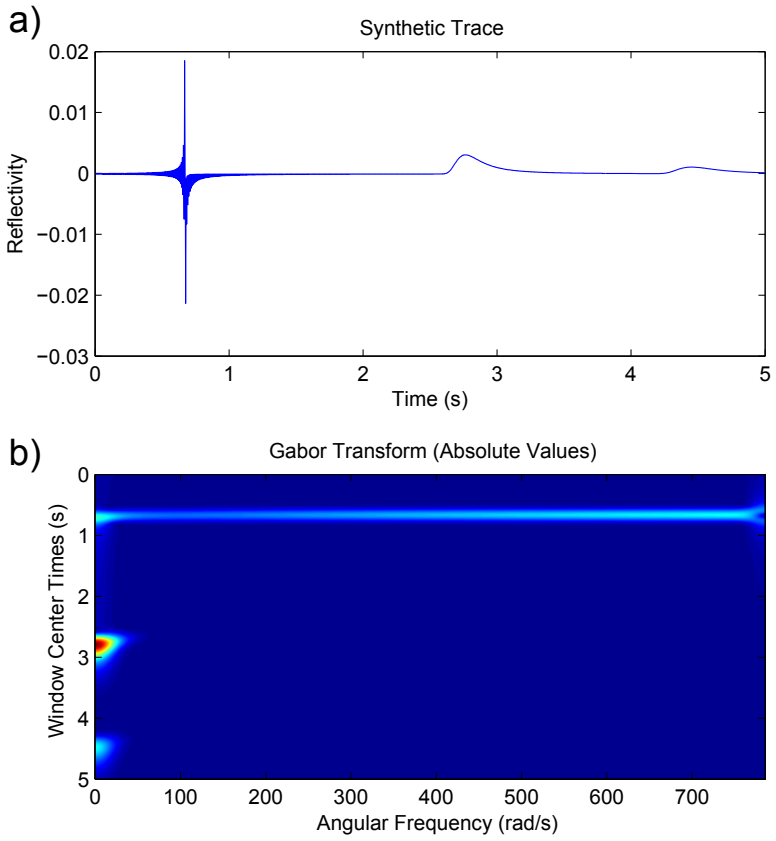

FIG. 1. Trace from our velocity and Q model and its corresponding Gabor transform. (a) The signal we are analyzing arrives at around 0.7 s, while additional signals at $\sim$ 2.8 and 3.5 s are included to ensure we are only analyzing part of the signal. (b) Absolute value of the Gabor transform of the trace shown in (a).

$$k = \frac{\omega}{c}\left(1 + \frac{i}{2Q} - \frac{log(\omega/\omega_r)}{\pi Q}\right) \tag{1}$$

Our models consist of an overburden of nearly elastic material (Q=10^6) overlaying a slightly faster, attenuative layer with a Q value which we vary between 5 and 10 throughout our tests. Additionally, there are two more layers beneath the second layer in order to model separate reflections that may be recorded in a trace and to ensure that the time-frequency analysis is being localized properly around the event. These reflections don't interfere with the reflectivity estimates unless they are too close in arrival time to the signal being analyzed (see the "close reflectors" section for a demonstration of the effects).

Our source is impulsive, which is applicable when the source wavelet has been deconvolved from a trace or when the upgoing wave has been divided by the downgoing wave. The synthetic trace generated using this source and our subsurface model can be seen in Figure 1a.

To retrieve reflectivity as a function of frequency from our trace, we first Gabor trans-

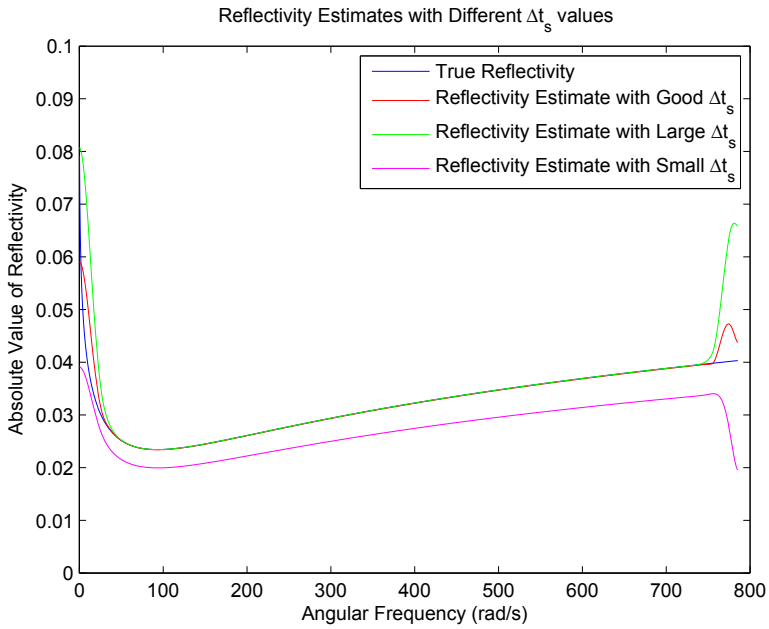

FIG. 2. Effect of summation size, Δt_s, on R(ω) estimate. The value should not be too small because then some of the signal will not be incorporated, or too large, because then more information not associated with the signal will contaminate the results.

form (using a Gabor transform code supplied by CREWES) the signal (the result is shown Figure 1b) and then sum the absolute values of the frequencies at each time and find the maximum of the total frequencies in order to determine the arrival time of the largest component of the signal. While this is not the arrival time of *all* of the signal, for simplicity, when referring to the arrival time henceforth, this is the time which we are referencing. When there are multiple events, we only find the maximum within the interval in which we are interested.

Due to dispersion, the reflections, as measured at the surface, are no longer impulsive and so the notion of an exact arrival time is compromised. This is especially true the longer the wave travels through a dispersive material, as can be seen by the larger widths of the second and third reflections than the first reflection in Figure 1a. Because of this spread of the signal in the time-domain, the spectrum of the Gabor transform at the calculated arrival time cannot be used by itself; the spectra calculated for nearby times in the Gabor transform need to be included as well. While theoretical work could be done to calculate an optimal weighting of each of the spectra that are close in time to the arrival time, this report is for proof of concept and our results for this will be empirical.

We tested a few summation schemes where we sum across the rows (times) of the Gabor transform within a summation time interval, Δt_s, of the arrival time on either side. Because the Gabor transform was already normalized so that summing the windows is unity for any given time, we did not need to divide by a factor to get the correct amplitude for the spectral content. The size of Δt_s, however, is a parameter that needs to be carefully chosen. It needs to be large enough that it captures the low-frequency spectral content of the signal, but making it too large can cause it to capture information at times away from the arrival

time, i.e. at times when there may not be signal arriving. Because the normalization factor is inversely related to the width of the Gaussian windows in the Gabor transform, Δt_s needs to be proportional to the window size used in the Gabor transform. Another explanation for this proportionality is that larger windows incorporate signal at larger lag times, so they need to be summed for larger lag times in order to incorporate all the information from the signal. Figure 2 shows results from a couple different Δt_s summation sizes using the Gabor spectrum from Figure 1b. Setting Δt_s too small underestimates reflectivity while setting it too large includes extra signal, in this case mostly at very low and very high frequencies.

For simplicity, R(ω) was first estimated using the absolute values of the frequency spectrum. In order to calculate the real component of R(ω), phase effects have to be removed. Figure 3a and b illustrate what happens if the real component of the Gabor transform is analyzed without accounting for phase effects. Because the first reflection approximates a delta function at a non-zero time, its spectrum approximates a complex exponential and so the real and imaginary components of its spectrum oscillate with frequency. Multiplying the signal by $e^{-it_a\omega}$ in the frequency domain, where t_a is the arrival time of the signal, should remove these effects. It should be noted that it is important that t_a is as accurate as possible. Using a t_a value that is slightly inaccurate will introduce an incorrect low-frequency component to R(ω) which will slightly change its slope. Because the slope of R(ω) will be used in the next section to invert for Q, it is important that it is as accurate as possible.

In order to ensure that t_a is as accurate as possible, we incorporate some of our prior knowledge about the characteristics of the R(ω) curve. Innanen (2011) expands R(ω) as a series in a_c and a_Q, and for an incoming wave at normal incidence to an interface finds

$$R(\omega) = \left(\frac{1}{4}a_c - \frac{1}{2}F(\omega)a_Q\right) + \left(\frac{1}{8}a_c^2 + \frac{1}{4}F^2(\omega)a_Q^2\right) + ... \tag{2}$$

where

$$a_c = 1 - \frac{c_0^2}{c^2}, \tag{3}$$

$$a_Q = \frac{1}{Q}, \tag{4}$$

and

$$F(\omega) = \frac{i}{2} - \frac{1}{\pi}log\left(\frac{\omega}{\omega_r}\right). \tag{5}$$

c_0 and c are the wavespeeds of a wave travelling through the medium of incidence and the target medium at a reference frequency, ω_r.

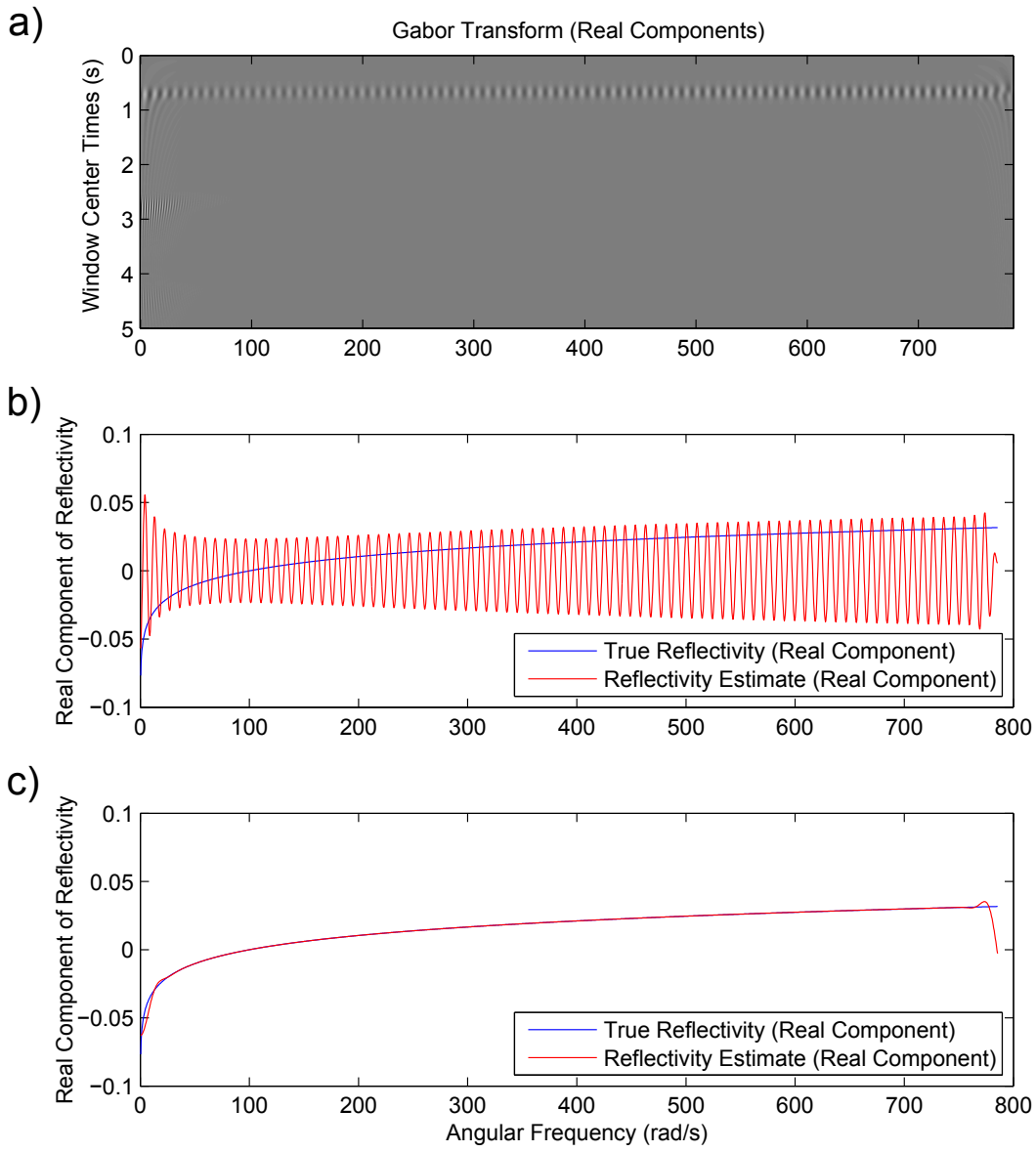

FIG. 3. Removal of phase effects in the real component of the signal. The oscillations of the real component of the Gabor transform with frequency in (a) causes an oscillatory Re reflectivity estimate in (b). (c) Multiplying the Re reflectivity estimate by $e^{-it_a\omega}$ removes these effects.

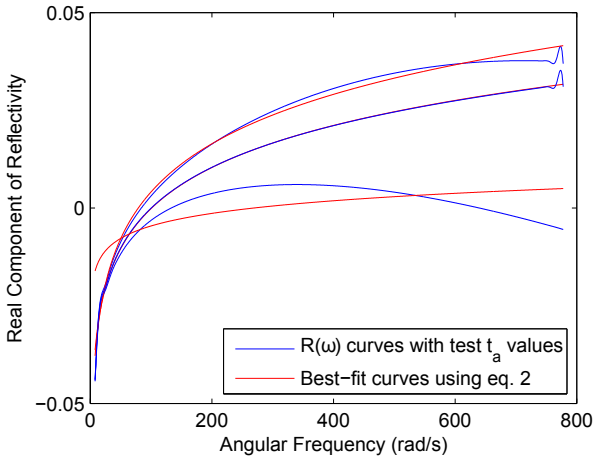

FIG. 4. The blue curves are R(ω) curves with phase effects removed for various test values of t_a (The middle R(ω) curve is the curve using the correct value of t_a). The red curves are the curves that best fit the test curves using first and second order terms of equation 2. Multiplying by the wrong $e^{-i\omega t_a}$ term results in a curve that cannot be well described by equation 2 and is not realistic physically.

For ω_r we use the highest frequency in our synthetics (the Nyquist frequency). It should be noted that the seismic velocities listed throughout this report are velocities for waves of this frequency (a stated velocity has to have an associated frequency since, due to dispersion, signals at different frequencies travel with different velocities).

It can be seen that equation 2 generates a logarithmic term that will be shifted up or down depending on a_c. In order to incorporate this knowledge into our workflow, we assume that our reflectivity curve should fit equation 2 well. Our process thus tests multiplying our R(ω) estimates containing phase effects (such as in Figure 3b) by $e^{-i\omega t_a}$ for a range of t_a values varying from 95% to 105% of the arrival time of the largest component of the signal. We then input each of these test curves into equation 2 (just using the first two orders of terms listed in the series) and solve for a_c and a_Q using the nonlinear least squares trust-region-reflective algorithm in MATLAB and see which t_a value yields the smallest L2-misfit against the best-fitting R(ω) curve. This was used to effectively remove the phase effects from Figure 3b to Figure 3c. In solving for a best-fitting curve and calculating the L2-misfit, we only use the middle 98% of the R(ω) estimate due to the lower accuracy of very low and very high frequency content when using a "medium-sized" Gabor transform window. A few of these tests and their best fitting curves can be seen in Figure 4, where the results using the t_a time that has the lowest L2-misfit as well as t_a values of $\pm 0.2\%$ of the best t_a time are shown. A small difference in t_a can clearly have a big effect.

From equation 4, we can obtain Q for the second layer using the a_Q value from the best-fitting R(ω) curve for the best-fitting t_a. Because the Q estimates were very close to the input Q values, the errors (our Q estimate minus the input Q value) were plotted instead of the actual estimates (Figure 5a). We also calculated and plotted errors of Q estimates for small (Figure 5b) and large (Figure 5c) velocity contrasts across the first interface.

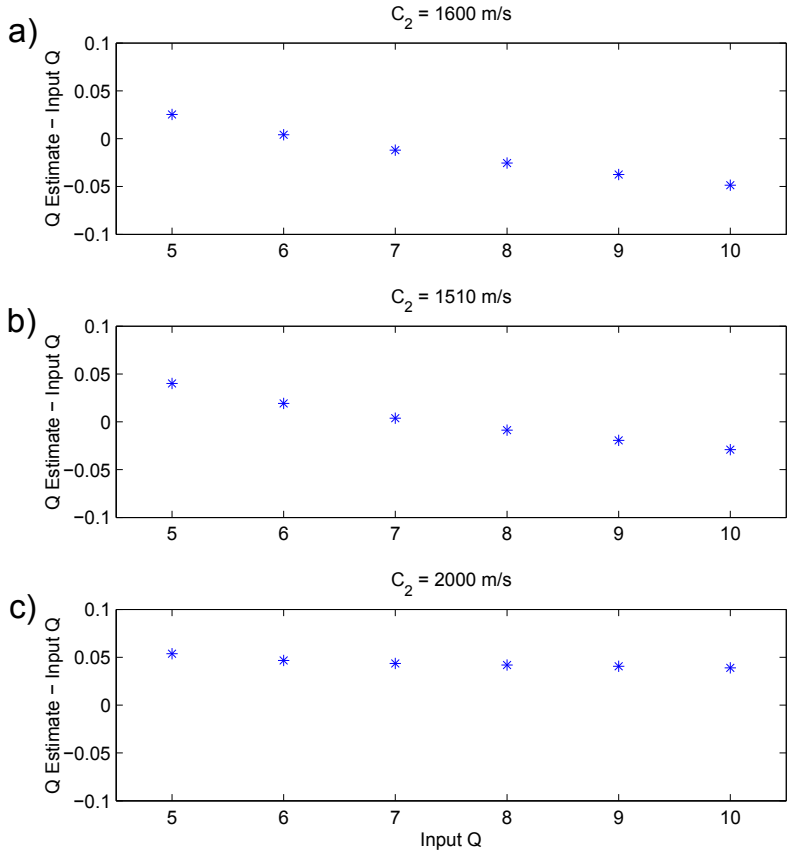

FIG. 5. Errors in Q estimates for 3 different velocities of the second layer. The top layer has a velocity of 1500 m/s. Q was accurately estimated for our original model (a), and using small (b) or large (c) velocity contrasts did not negatively affect the Q estimation results.

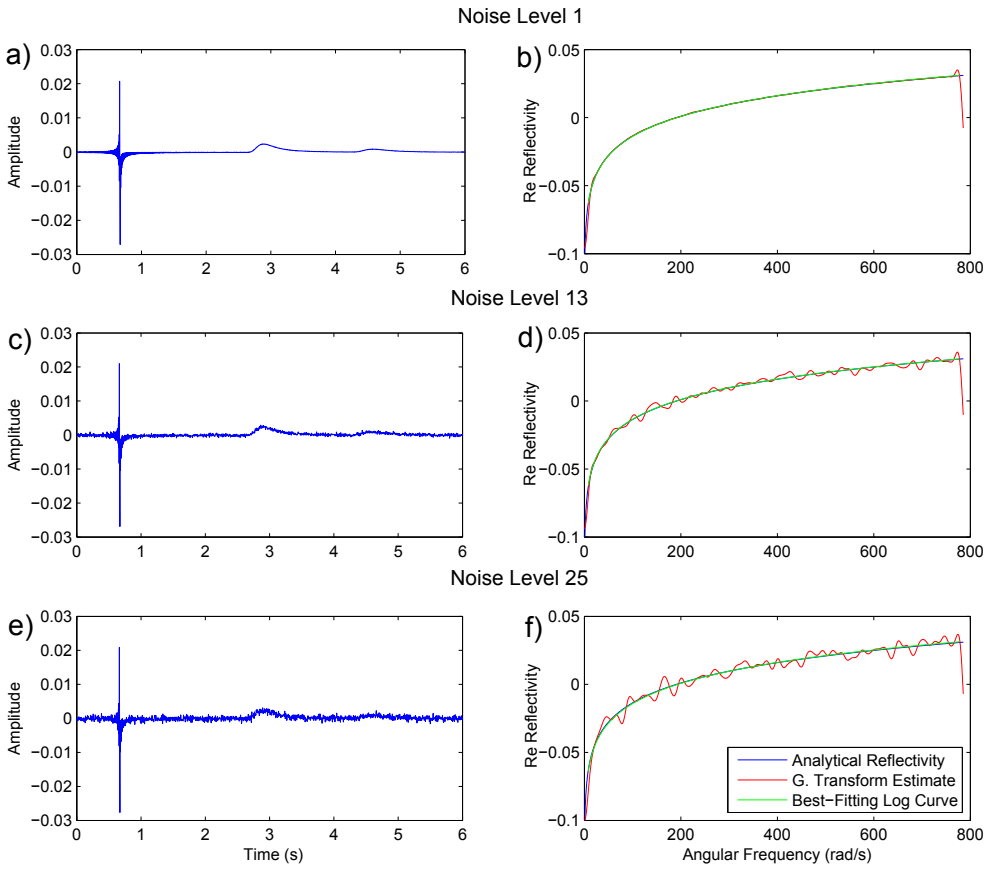

FIG. 6. Noisy traces and their respective reflectivity estimates. (a), (c), and (e) Synthetic traces with increasing levels of white noise added. (b), (d), and (f) Real R(ω) estimates and their best-fitting curves, using equation 2, plotted against the true (real component of) reflectivity.

NOISE TESTS

When using real data, many problems not encountered in simple synthetic models will be introduced. One of these additional problems will be noise, which overlays recorded signal. Noise is often signal-generated and/or contains dominant frequencies. Modeling noise for data sets used in Q analysis is, however, beyond the scope of this report. Because noise encountered in seismic data sets is often close to constant along part of the bandwidth of its power spectrum, adding white noise to synthetics can be useful for preliminary noise analysis, and this is what we test in this report.

We added 25 increasing levels of white noise to synthetic traces generated using the original model. Traces after the addition of noise can be seen for noise levels 1, 13, and 25 in Figure 6a, c, and e. Our method was used to estimate Q for input Q values of 5 to 10, and then this process was repeated 10 times at each noise level (adding different random noise to the clean trace each time). In Figure 6b, d, and f the reflectivity curves, the reflectivity estimates from the Gabor transform, and the best-fitting curve using equation 2 are plotted for noise levels 1, 13, and 25, respectively.

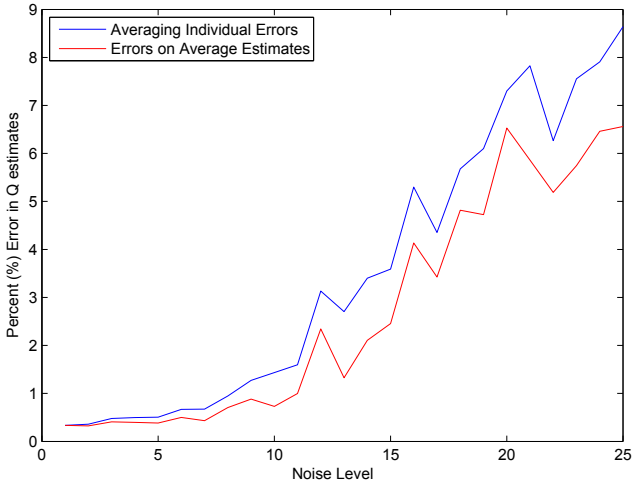

FIG. 7. Percent errors in Q estimates using noisy data. 10 noisy traces were created for each Q value at each noise level. In blue is the average percent error in Q estimates for 25 increasing levels of white noise added to synthetic traces. In red is the percent error in the Q estimate when averaging the same Q estimates across the 10 noisy traces at a given noise level for a given Q value.

Using the 6 input Q values, we measured the error in Q estimates for a given noise level, and with each estimate the absolute value of the error was divided by the true Q value to get a percent error. This process was repeated 10 times and the percent errors were averaged across the 10 repetitions. The results of this for each of the 25 noise levels are shown in blue in Figure 7. To see if stacking Q estimates from 10 traces could reduce the error, for each input Q value and level of noise we averaged the 10 Q estimates and used this for our percent error. This averaged result is shown in red in Figure 7 and it demonstrates that the random noise is not averaging out effectively when stacking Q estimates. The reason behind this will be discussed in the next paragraph, but it should also be noted that stacking traces to lower the noise and then estimating Q could eliminate this problem.

When viewing the Q estimate results with higher noise levels, we discovered that the Q estimates were much more often overestimated than underestimated, leading to systematically high Q estimates, even when averaging using many noisy traces. Also, this overestimation of Q was often an error much larger than to be expected given the level of noise. In Figure 8, the red curve is the resulting R(ω) estimate from a single noisy trace using our standard framework, and the green curve is the clean trace processed using the same best-fitting time that was found for the noisy trace. This reflectivity curve is clearly above the true reflectivity curve (dark blue), which is because the wrong arrival time for t_a gave a lower L2 misfit between the reflectivity estimate and the best-fitting curve and was chosen. When forcing the algorithm to use the correct value for t_a for the same trace, the reflectivity curve (magenta) is then close to the true reflectivity, and a clean trace processed in the same way (cyan) overlays the true reflectivity. Thus, by causing the procedure to choose the wrong arrival time, the noise introduces a low frequency component to the R(ω) estimate, which affects the Q estimate.

The noise test was run again, but this time with t_a values fixed at the true arrival time

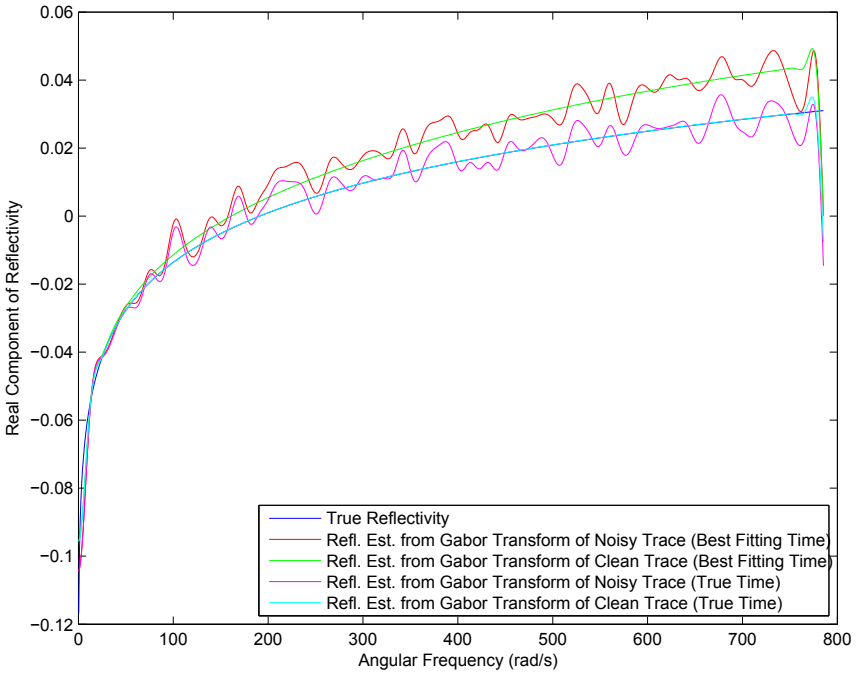

FIG. 8. Wrong t_a estimate due to noise. Due to the noise, t_a was misestimated, resulting in a noisy R(ω) curve with the wrong slope (shown in red) and if a clean trace is processed using the same best-fitting time found for the noisy trace, it will not match the true reflectivity (green vs. dark blue). If the same noisy trace is processed using the correct t_a (shown in magenta), it better fits the true reflectivity. Using the clean trace with the correct time is shown for comparison (cyan).

and the results are shown in Figure 9. All the noisy results were improved and the stacking has a much larger effect now that outliers are less present in the averaging.

CLOSE REFLECTORS

One of the problems that naturally arises with using an R(ω) estimate from a reflection to infer Q is that alternate arrivals may overlay or lie close to the signal in which one is interested. When such a situation occurs, part of the reflectivity that is measured comes from a different arrival.

We tested the effect of this proximity of signals by moving the second interface progressively closer to the first interface and measuring the effects on R(ω) and Q estimates. Figure 10a-d shows synthetic traces for separation distances between the top two reflecting interfaces of 100, 200, 300, and 400 m (for reference, the velocity between the two layers at the reference frequency, ω_r, is 1600 m/s). The red Gaussian plotted on top of the trace is the size of the Gaussian window we used in the Gabor transform previously as well as in the Gabor transforms in Figure 10. Just by looking at the traces it can be seen that there is going to be a problem as the two reflectors move closer together in depth and the arrivals of their reflections become closer in time. Also, it should be remembered that the Gabor transform moves the Gaussian window and the plot of the window on top of the traces is only an indication of where the window will be for one row of the Gabor transform.

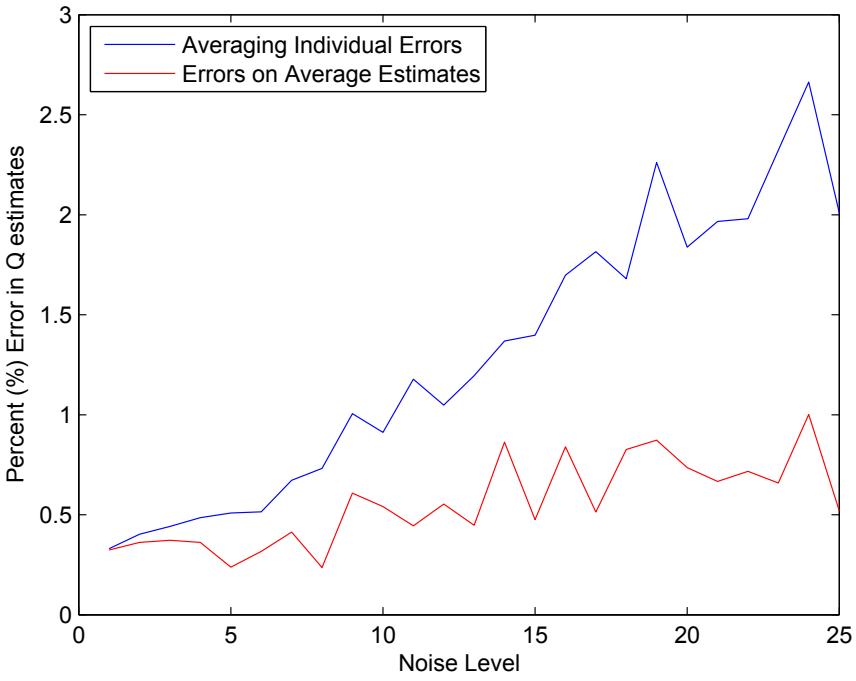

FIG. 9. Percent errors when forcing the correct t_a. These are the percent errors using the same procedure as in Figure 7, except t_a was fixed to the correct value instead of being calculated.

Below the traces are the Gabor transforms, R(ω) estimates, and best-fitting curves to the R(ω) estimates for each trace. When calculating R(ω) for Figure 10i, the arrival time estimate was calculated finding the row with the maximum of the sum of absolute values using only times prior to the arrival of the second reflection. Otherwise, our method would choose the second reflection as the signal to analyze, since it is now stronger as seen by its large amplitude in Figure 10a.

As the two signals become close in time, the R(ω) curves become less accurate due to their inclusion of unwanted signal. This can be seen in the slight oscillations of the R(ω) estimate in Figure 10k, and the large oscillations and inaccurate slope of the R(ω) estimates in Figure 10i and j.

In an attempt to isolate only the signal in which we are interested, we also performed the same procedure on the same four models, but made the widths of the Gaussian windows in the Gabor transform a fourth of their previous size (and divided the region of summation, Δt_s, by a factor of four as well). The results with this change can be seen in Figure 11, and the new size of the Gaussian window used can be seen in Figure 11a, b, c, and d. Once again, we had to restrict the region for which the initial arrival time estimate could be made for Δz = 100 m, which was done to create Figure 11a.

Using a smaller window can clearly help isolate a signal when two signals are close in time. The Q estimates for the two approaches are shown for the four separation distances of the reflectors in Figure 12. Using the original window clearly leads to incorrect Q estimates when the two signals were close enough to each other (Figure 12a and b), but gives slightly

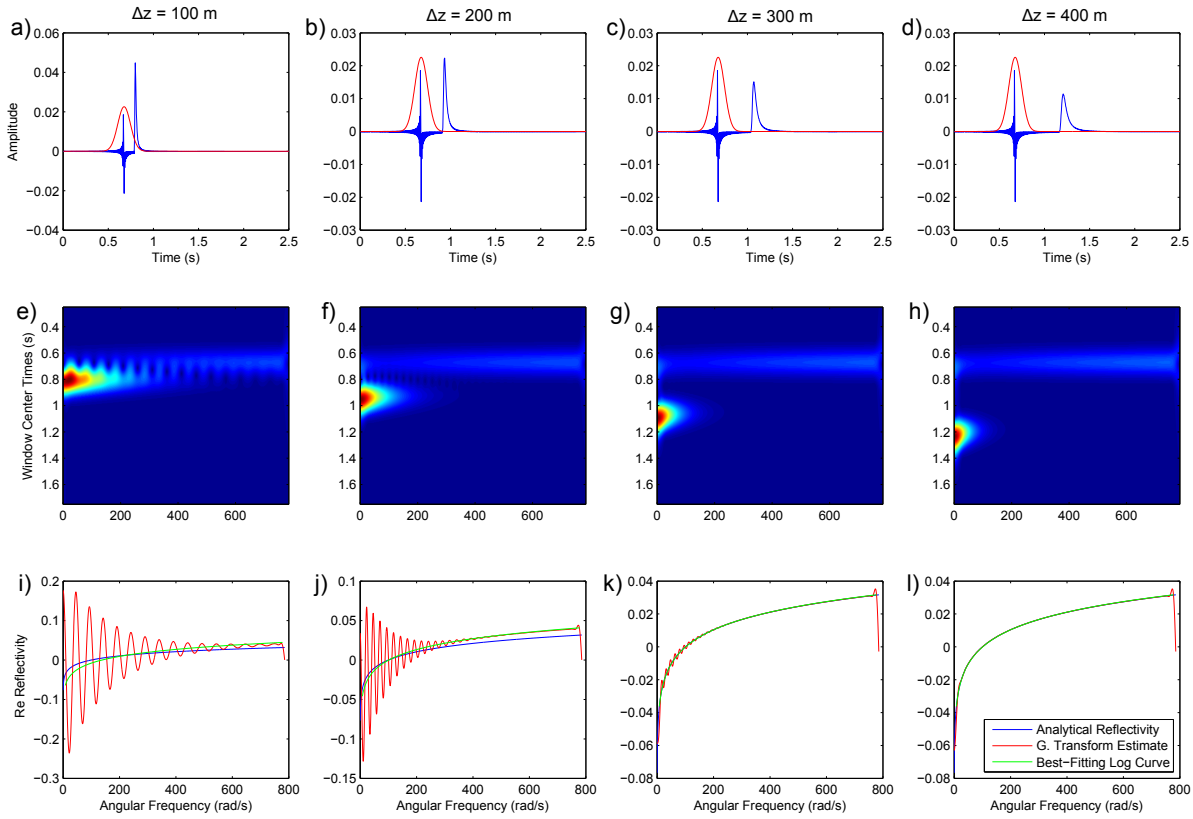

FIG. 10. Analysis using our standard Gaussian window size for closer reflectors. (a-d) show traces for two reflections separated by distances of 100, 200, 300, and 400 m. In red is the size of the Gaussian window used in our Gabor transforms for this analysis. (e-h) show the Gabor transforms and (i-l) show the R(ω) estimates, and their best-fit curves, for the traces above them.

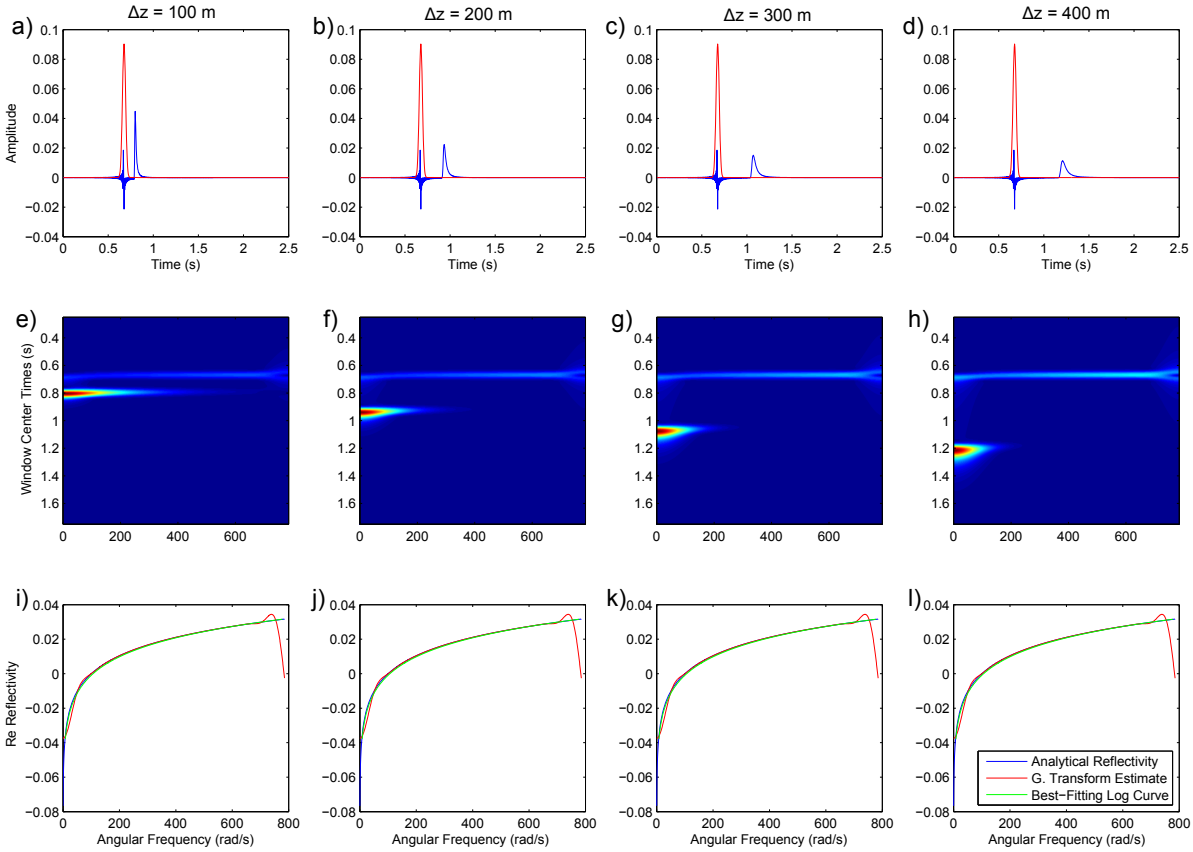

FIG. 11. Analysis using a thinner Gaussian window for closer reflectors. This is the same analysis as in Figure 10, but with a Gaussian window a quarter the width and a Δt_s value a quarter as large as in our standard procedure.

more accurate results when the smaller window is not needed (Figure 12c and d), which can be explained by the smaller window's inability to capture all of the information from the signal (especially at low frequencies).

CONCLUSIONS

Future research in this subject has many opportunities to improve the procedure. Since the value of t_a strongly influences estimation of Q in our method, determining it accurately is very important, and creating an algorithm which more accurately determines it should yield more stable results, especially in the presence of noise. While we only tested combining noisy data sets by averaging their Q estimates, their information could also be combined to determine t_a prior to inferring R(ω). There may also be methods for removing phase effects which are more stable than multiplying by a complex exponential. Additionally, it should be noted that while we removed these phase effects to analyze the real component of the reflectivity, the complex component of the reflectivity was never used even though it contains information about the interface.

We used the Gabor transform, which is a short-time Fourier transform with a Gaussian

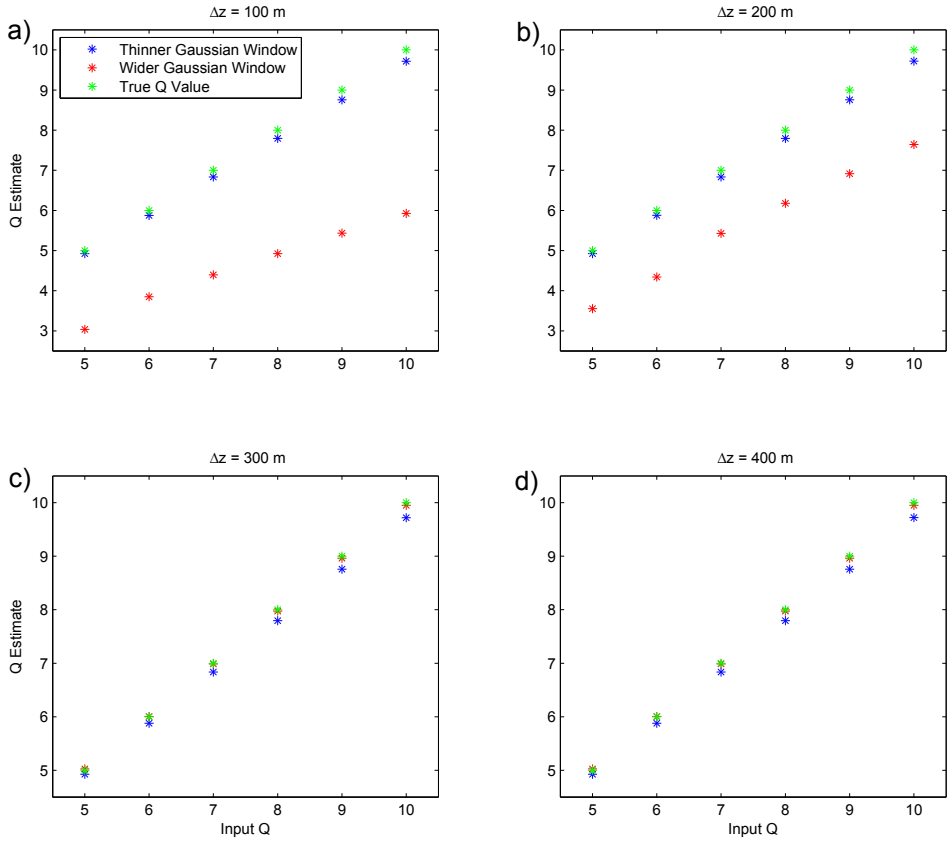

FIG. 12. Q estimates for closer reflectors. These Q estimates were obtained using the results shown in Figures 10 and 11. (a & b) Using the thinner Gaussian window resulted in more accurate Q estimates for the very close reflectors. (c & d) Using the wider Gaussian window resulted in slightly more accurate Q estimates for the reflectors separated by a larger distance.

window, in our method. It is possible that other windows will yield better results and so this method should be tested using other short-time Fourier transforms, specifically when there are multiple events arriving close together in time.

Using the Gabor transform to estimate frequency-dependent reflectivities is clearly an approach that can be used to accurately estimate Q in synthetics under a variety of conditions. Due to this success, we believe that the method should be tested using real data sets in order to assess its effectiveness in estimating Q in real data compared to other methods.

ACKNOWLEDGMENTS

We would like to thank CREWES for providing Gabor transform codes and for supporting this project. Additionally, we would like to thank CREWES and CREWES sponsors for funding this work.

REFERENCES

Aki, K., and Richards, P. G., 2002, Quantitative seismology: Theory and methods: University Science Books.

Bird, C., 2012, Amplitude-variation-with frequency (AVF) analysis of seismic data over anelastic targets: M.Sc. thesis, University of Calgary.

Cheng, P., and Margrave, G., 2012, Estimation of Q: a comparison of different computational methods: CREWES Research Report, **24**.

Hargreaves, N. D., and Calvert, A. J., 1991, Inverse Q filtering by Fourier transform: Geophysics, **56**, No. 4, 519–527.

Innanen, K. A., 2011, Inversion of the seismic AVF/AVA signatures of highly attenuative targets: Geophysics, **76**, No. 1, R1–R14.

Kuster, G. T., and Toksöz, M. N., 1974, Velocity and attenuation of seismic waves in two-phase media: Part I. theoretical formulations: Geophysics, **39**, No. 5, 587–606.

Mavko, G. M., and Nur, A., 1979, Wave attenuation in partially saturated rocks: Geophysics, **44**, No. 2, 161–178.

Pride, S. R. et al., 2003, Permeability dependence of seismic amplitudes: The Leading Edge, **22**, No. 6, 518–525.

Vasheghani, F., and Lines, L. R., 2009, Viscosity and Q in heavy-oil reservoir characterization: The Leading Edge, **28**, No. 7, 856–860.